Anti-epileptic mechanism of isopimaric acid from *Platycladi cacumen* based on network pharmacology, molecular docking and biological validation

YAN WANG[1,2*], YUN WANG[1-3*], CHANG LI[1-3], DONG LIU[2], YI CAI[1-3] and QIFU LI[1-3]

[1]Department of Neurology, The First Affiliated Hospital of Hainan Medical University, Haikou, Hainan 570102, P.R. China; [2]Engineering Research Center of Tropical Medicine Innovation and Transformation of Ministry of Education, International Joint Research Center of Human-Machine Intelligent Collaborative for Tumor Precision Diagnosis and Treatment of Hainan Province, Hainan Key Laboratory for Research and Development of Tropical Herbs and Haikou Key Laboratory of Li Nationality Medicine, School of Pharmacy, Hainan Medical University, Haikou, Hainan 571199, P.R. China; [3]Key Laboratory of Brain Science Research and Transformation in Tropical Environment of Hainan Province, Hainan Medical University, Haikou, Hainan 571199, P.R. China

Received January 18, 2024; Accepted April 15, 2024

DOI: 10.3892/etm.2024.12637

Abstract. *Platycladi cacumen* (PC) is derived from the dry twigs and leaves of *Platycladi orientalis* (L.) Franco and exerts anti-epileptic effects. However, its mechanism of action remains unknown. The present study explored the potential anti-epileptic components and mechanisms of PC. The primary active components and targets of PC were analyzed using network pharmacology and a lipopolysaccharide (LPS)-induced murine microglial cell line (BV2) was used to confirm anti-epileptic effects by detecting reactive oxygen species (ROS), apoptosis, inflammatory markers, cell migration and signaling pathways. A total of 13 core active components showed druggable properties, of which deoxypicrop odophyllotoxin, hinokinin and isopimaric acid (IPA) were predicted to cross the blood-brain barrier. In total, 255 potential targets of these three compounds were predicted using SwissTargetPrediction and Similarity Ensemble Approach websites and 150 were associated with epilepsy. *In vitro* experiments confirmed that IPA significantly inhibited LPS-induced microglial oxidative stress and inflammation by decreasing the migration area, cellular ROS content, lactate dehydrogenase release and early phase of apoptosis. IPA also increased the mRNA expression of anti-oxidative enzymes (superoxide dismutase-1 and -2) and suppressed inflammatory cytokines (interleukin-1β and tumor necrosis factor-α). Furthermore, IPA phosphorylated AKT and mTOR proteins. Taken together, the present findings suggested that IPA is a potential anti-epileptic compound derived from PC.

Correspondence to: Professor Yi Cai or Professor Qifu Li, Department of Neurology, The First Affiliated Hospital of Hainan Medical University, 31 Longhua Road, Haikou, Hainan 570102, P.R. China
E-mail: caiyi66817616@163.com
E-mail: lee-chief@163.com

*Contributed equally

Key words: *Platycladi cacumen*, isopimaric acid, network pharmacology, lipopolysaccharide-induced BV2 cell, inflammation, AKT, mTOR

Introduction

Epilepsy is a common neurological disorder caused by abnormal brain discharge, characterized by recurrent limb twitching and loss of consciousness. It affects ~1% of the global population. Currently, antiseizure medication (ASM) is the primary treatment for epilepsy (1). However ~30% of cases remain medically intractable, resulting in a heavy economic burden on patients and society (2). Therefore, it is necessary to develop novel ASMs that effectively control seizures.

Platycladi cacumen (PC), a widely used traditional Chinese medicine, is derived from dry twigs and leaves of *Platycladi orientalis* (L.) Franco. It is traditionally used to cool blood, stanch bleeding, dispel pathogenic winds, remove dampness, eliminate phlegm and raise hair and blacken hair (3). Recently, PC was shown to exert anti-inflammatory, antioxidative and neuroprotective effects (4). Aqueous extracts of PC suppress lipopolysaccharide (LPS)-induced intestinal inflammation by increasing colon length and inhibiting fecal occult blood, severe diarrhea and enteritis (5). PC carbonisata-derived nanoparticles inhibit ulcerative colitis induced by 2,4,6,-trinitrobenzene-sulfonic acid in rats by decreasing tumor necrosis factor-α (TNF-α) and interleukin-6 and upregulating interleukin-10 (4). Furthermore, denuded mice treated with water extract of PC for 4 weeks exhibit increased hair growth with increasing hair bulb size and dermis and epidermal thickness (6). A similar effect was found with volatile oil extracts of PC (7). Furthermore, PC exerts renoprotective effects by targeting renal organic anion transporters 1 and 3 to inhibit protein activity (8). A total of 43 compounds have been extracted and separated by 75% methanol from PC and grouped as organic acids, flavonoids, phenylpropanoids, volatile oils and tannins (9). Among them,

myricitrin, quercitrin and amentoflavone are the primary compounds (10) that ameliorate liver ischemia-reperfusion and (11) kidney injury (11) and inhibit platelet activation in arterial thrombosis (12) and human breast cancer (13).

The efficacy of PC against epilepsy has been reported in 'Effective Prescription for Epilepsy Treatment' (14). However, its anti-epileptic components and underlying mechanisms remain unclear. Therefore, in the present study, the anti-epileptic compound PC was explored using network pharmacology and *in vitro* experiments.

Materials and methods

Construction of an 'Herbs-Components-Targets' (H-C-T) network. The Traditional Chinese Medicine System Pharmacology Database (TCMSP) was used to identify the active ingredients of PC (15), of which, the components whose toxicokinetic absorption, distribution, metabolism and excretion (ADME) adhered to oral bioavailability (OB) ≥30% and drug-likeness (DL) ≥0.18 were defined as the main compounds. Druggable compounds that may cross the blood-brain barrier (BBB) as predicted by SwissADME (swissadme.ch/index.ph) were further used to identify targets on the SwissTargetPrediction (SWISS; new.swisstargetprediction.ch/) and similarity ensemble approach (SEA; sea.bkslab.org/) websites by using relative Canonical Simplified Molecular Input Line Entry System (SMILES) numbers.

Genes associated with epilepsy were obtained from GeneCards (version 4.9.0; genecards.org/). Overlapping genes between targets of the druggable compounds and epilepsy-associated targets were retrieved using VENN map (bioinformatics.psb.ugent.be/webtools/Venn/). The protein-protein interaction (PPI) network was analyzed using the protein-protein interaction networks functional enrichment analysis online tool (STRING; string-db.org/) and core genes were obtained using the CytoNCA of Cytoscape3.9.1 (cytoscape.org/) with the criteria of two-fold the median value of degree centrality (DC), median values of betweenness centrality (BC) and closeness centrality (16). The H-C-T network of PC was constructed using Cytoscape3.9.1.

Gene functions and pathway analysis. Gene Ontology (GO) biological process, cellular component and molecular function and Kyoto Encyclopedia of Genes and Genomes (KEGG) pathways were analyzed among the overlapping genes using the web-based tool DAVID v6.8 (david.ncifcrf.gov/tools.jsp) (17). $P<0.05$ (Bonferroni-corrected) was considered to indicate statistical significance.

Cell culture and proliferation assay. The murine microglial cell line BV2 was purchased from Procell Life Science & Technology Co., Ltd. and cultured in high-glucose Dulbecco's modified Eagle's medium (DMEM; Gibco; Thermo Fisher Scientific, Inc.) with 10% fetal bovine serum (Clark Bioscience) and 1% streptomycin/penicillin (Biosharp Life Sciences) in a humidified incubator with 5% CO_2 at 37˚C.

Cell proliferation was assessed using Cell Counting Kit-8 (CCK8; Dojindo Molecular Technologies, Inc.). Briefly, cells ($1x10^4$/ml) were seeded and cultured in 96-well microplates for 24 h. Cells were treated with isopimaric acid (IPA, Sigma-Aldrich; Merck KGaA; 0.1, 1.0, 10.0, 100.0 and 1,000.0 μM) for 24 h, followed by incubation with 10 μl CCK8 reagent for 1 h all at 37˚C. Absorbance was measured by a microplate reader (BioTek Instruments, Inc.; EPOCH2NS) at 450 nm. Survival rate was calculated as follows (18): Survival rate %=absorbance of IPA/absorbance of control x100%.

Wound healing assay. Confluent BV2 cells (90%) were scratched using a pipette tip and washed three times with PBS to remove non-adherent cells. The cells were incubated with LPS (1 μg/ml; Sigma-Aldrich; Merck KGaA) in the presence or absence of 0.0, 0.1, 1.0, 10.0 or 100.0 μM IPA for 24 h ay 37˚C. Images of the central cell-free zone before and after treatment were obtained by light field microscopy (magnification, x200; Zeiss X-Cite; Carl Zeiss AG) (19). The migratory area was calculated as follows: Migratory area (%)=[(area at 0 h - area at 24 h)/area at 0 h] x100%.

LDH assay. The medium of cells treated with LPS in the presence or absence of IPA was collected to determine the released LDH content using assay kits (no. A020-2-2; Nanjing Jiancheng Bioengineering Institute) as previously described (20).

Flow cytometric analysis of cellular reactive oxygen species (ROS). Following treatment with LPS in the presence or absence of IPA for 24 h, cells were incubated at 37˚C with 10 μM 2',7'-dichlorofluorescin diacetate (MedChemExpress) diluted in DMEM for 30 min in the dark. Images were captured using a fluorescence microscope (Zeiss X-Cite; Zeiss AG) and mean intensity was measured using a flow cytometer (NovoCyte; Agilent Technologies, Inc.) in the fluorescein isothiocyanate (FITC) channel.

Annexin V-FITC/propidium iodide (PI) analysis for apoptosis. BV2 cells were digested 37˚C for 5 min using trypsin, followed by incubation with Annexin-FITC and PI for 5 min at room temperature (Boster Biological Technology). Fluorescence intensities were detected using a flow cytometer (NovoCyte) with FITC and PI channels, as previously described (21). A total of four populations of cells were distinguished: Viable (no staining), early apoptosis (Annexin V^+PI^-), late apoptotic cells (Annexin V^+PI^+), and necrotic (Annexin V^-PI^+) cells. Apoptosis was determined as early + late apoptosis.

Determination of mitochondrial membrane potential (MMP). Cells were treated with IPA and LPS for 24 h, followed by incubation with 500 μl JC-1 working solution in the dark (Beyotime Institute of Biotechnology) for 20 min at 37˚C. Images were obtained using a fluorescence microscope in the FITC and PI channels (magnification, x200; Zeiss X-Cite; Carl Zeiss AG).

Reverse transcription-quantitative (RT-q)PCR. Total RNA from BV2 cells was extracted using TRIzol (Invitrogen; Thermo Fisher Scientific, Inc.) and reverse-transcribed to cDNA using MonScript Reverse Transcriptase (cat. no. MR05101; Monad Biotech Co., Ltd.), followed by SYBR Green PCR (cat. no. MQ00401; Monad Biotech Co., Ltd.), according to the manufacturer's protocol as previously described (21). Relative

Table I. Sequence and length of primers.

Gene	Forward, 5'→3'	Reverse, 5'→3'	Length, bp
Actin	CCACAGCTGAGAGGGAAATC	AAGGAAGGCTGGAAAAGAGC	193
SOD-1	CCATCAGTATGGGGACAATACA	GGTCTCCAACATGCCTCTCT	109
SOD-2	GACCCATTGCAAGGAACAA	GTAGTAAGCGTGCTCCCACAC	69
IL-1β	TGCCACCTTTTGACAGTGATG	GGAGCCTGTAGTGCAGTTGT	351
TNF-α	GTAGCCCACGTCGTAGCAA	GTGAGGAGCACGTAGTCGG	191
Arg-1	GAACACGGCAGTGGCTTTAAC	TGCTTAGCTCTGTCTGCTTTGC	155

SOD, superoxide dismutase; Arg, arginase.

Table II. Antibody information.

Antibody	Supplier	Cat. no.	Dilution
Rabbit anti-TNF-1α	Cell Signaling Technology, Inc.	8184	1:1,000
Rabbit anti-IL-1β	Cell Signaling Technology, Inc.	12703S	1:1,000
Mouse anti-AKT	Proteintech Group, Inc.	60203-2	1:5,000
Rabbit anti-p-AKT	Proteintech Group, Inc.	80455-1-RR	1:5,000
Rabbit anti-mTOR	Abcam	ab2732	1:5,000
Mouse anti-p-mTOR	Proteintech Group, Inc.	67778-1	1:2,000
Mouse anti-PI3Kα	Proteintech Group, Inc.	67071-1-lg	1:1,000
Mouse anti-PI3Kβ	Proteintech Group, Inc.	67644-1-lg	1:5,000
Rabbit anti-GAPDH	Proteintech Group, Inc.	10494-1-AP	1:6,000

PI3K, phosphatidylinositol 3-kinase; p-, phosphorylation.

expression levels of target genes were calculated based on the $2^{-\Delta\Delta Cq}$ method using actin as a reference housekeeping gene (22). The primer sequences are listed in Table I.

Western blotting. Total protein was extracted from BV2 cells using a cell lysis buffer (cat. no. P0013, Beyotime Institute of Biotechnology) with a phosphatase inhibitor, while concentrations of proteins were determined by bicinchoninic acid method (Wuhan Boster Biological Technology, Ltd.). Protein lysates (50 μg) were resolved by 10% sodium dodecyl sulfate-polyacrylamide gel electrophoresis and transferred onto a polyvinyl difluoride membrane (MilliporeSigma) via electroblotting. Each blot was blocked by QuickBlock (cat. no. P0256; Beyotime Institute of Biotechnology) for 15 min at room temperature and incubated with primary antibodies overnight at 4˚C (Table II). Membranes were incubated with horseradish peroxidase-conjugated secondary antibodies (Proteintech Group, Inc.; cat. no. 20000858; 1: 2,000; cat. no. 20000757; 1:5,000) for 1 h at 37˚C. The blots were visualized by the ChemiDoc XRS imaging system (Bio-Rad Laboratories, Inc.) with BeyoECL kit (cat. no. 081723240119; Beyotime Institute of Biotechnology) and quantified using ImageJ Software (v1.52a; National Institutes of Health).

Molecular docking. The crystallographic structure of AKT was obtained from the Protein Data Bank (PDB code: 4GV1) (23) and docking by using Schrödinger (version 2015) (24). Briefly, the Protein Preparation Wizard and Receptor Grid Generation modules were used to prepare the proteins. Ionization-generated possible states of the LigPrep module were set at a target pH of 7.0±2.0 to prepare IPA to dock flexibly into the ligand site using a Ligand Docking module in standard precision mode, as previously described (25).

Statistical analysis. Data are presented as the mean ± SD. Normally distributed data were analyzed using the Shapiro-Wilk test and one-way ANOVA followed by Dunn's post hoc test for multiple groups using GraphPad Prism (version 9.0.0; Dotmatics) (26). Non-normally distributed data were analyzed using Kruskal-Wallis test. $P<0.05$ was considered to indicate a statistically significant difference.

Results

Targets prediction of PC and visualization of H-C-T network. A total of seven primary compounds were obtained from the TCMSP, of which hinokinin, IPA and deoxypicropodophyllotoxin (DPT) exhibited the potential to cross the BBB (Table III; Fig. 1A). Based on SMILES numbers of these three components, 255 potential targets of PC were identified by target fishing from the SWISS and SEA databases, of which 150 were associated with epilepsy (Fig. 1B). These composite targets were input into STRING to construct a PPI network with connected targets (combined score >0.7), including 259 nodes and 308 edges

Table III. Characteristics of seven active constituents derived from PC.

ID no.	Molecule	MW (g/mol)	DL	OB, %	BBB-permeable
MOL000098	Quercetin	302.25	0.28	46.43	No
MOL000358	β-sitosterol	414.79	0.75	36.91	No
MOL000422	Kaempferol	286.25	0.24	41.88	No
MOL002005	Hinokinin	354.38	0.64	56.5	Yes
MOL002032	DNOP	390.62	0.40	40.59	No
MOL002034	(5aR,8aS,9R)-9-(3,4,5-trimethoxyphenyl)-5a,6,8a,9-tetrahydro-5H-isobenzofurano[5,6-f][1,3]benzodioxol-8-one (Deoxypicropodophyllotoxin)	398.44	0.83	52.70	Yes
MOL002039	Isopimaric acid	302.45	0.28	36.20	Yes

MW, molecular weight; DL, drug-like; OB, oral bioavailability; BBB, blood-brain barrier; DNOP, dioctyl phthalate.

(Fig. 1C). A total of 13 targets, including TNF, tumor protein (TP53), estrogen receptor 1 (ESR1), prostaglandin-endoperoxide synthase 2 (PTGS2), microtubule affinity regulating kinase 3 (MARK3), peroxisome proliferative activated receptor gamma (PPARG), caspase 3 (CASP3), B-cell lymphoma-2 (BCL2), glycogen synthase kinase 3 beta (GSK3B), mammalian target of rapamycin (mTOR), protein tyrosine phosphatase non-receptor type11 (PTPN11), sirtuin1 (SIRT1) and murine double minute 2 (MDM2) exceeded the values (two-fold of DC, median of BC and closeness centrality; Fig. 1D). Among these, BCL2, GSK3B, and mTOR are potential anti-epileptic targets for hinokinin; CASP3, mTOR, and SIRT1 for DPT; and TNF, TP53, ESR1, PTGS2, MAPK3, PPARG, PTPN11, and MDM2 for IPA. In particular, TNF showed the highest subgraph centrality value.

GO and KEGG enrichment analysis. GO and pathway enrichment analyses were performed for overlapping targets (150 genes) that were significantly enriched 'protein phosphorylation', 'negative regulation of apoptotic process', 'response to xenobiotic stimulus', 'protein autophosphorylation' and 'peptidyl-serine phosphorylation' in the biological processes. In terms of cellular component, the overlapping targets were enriched in the 'membrane raft', 'macromolecular complex', 'dendrite', 'cell surface', and 'receptor complex'. With respect to molecular function, the core targets were enriched in 'protein serine/threonine/tyrosine kinase activity', 'protein serine/threonine kinase activity', 'kinase activity', 'protein tyrosine kinase activity', and 'RNA polymerase II transcription factor activity, ligand-activated sequence-specific DNA binding' (Fig. 1E). A total of 150 genes were enriched in 140 pathways, of which 'pathways in cancer', 'PI3K-Akt signaling pathway', 'pathways of neurodegeneration-multiple diseases', 'cAMP signaling pathway' and 'MAPK signaling pathway' were the most enriched (Fig. 1F).

IPA inhibits elevation of ROS production and migration of murine microglia cells induced by glutamate and LPS. IPA serves a role in pathological processes, including antibacterial activity (27) and anti-NLR family, pyrin domain containing protein 3 (NLRP3) inflammasome (28) and anti-Alzheimer's disease effects (29,30). IPA activates large-conductance Ca^{2+}-activated K^+ channels (31,32) by targeting gamma-aminobutuyric acid (GABA) receptors to induce chloride ion currents (33). Therefore, it was hypothesized that IPA may be a might be a target compound to treat epilepsy. Hence, glutamate- and LPS-induced excitotoxicity and neuroinflammation in murine microglia cells BV2 were examined to determine the anti-epileptic effects of IPA, as previously described (34).

IPA (0.1-1,000.0 μM) was used to verify its effect on the survival of BV2 cells. Concentrations of IPA from 0.1 to 100.0 μM did not affect the survival rate of BV2 cells and were applied in subsequent experiments (Fig. 2A and B). BV2 cells treated with glutamate (5 mM) for 12 h and LPS (1 μg/ml) for 24 h notably suppressed the survival rate. However, co-administration of IPA did not improve the survival of BV2 cells (Fig. 2C and D) but significantly suppressed the production of ROS induced by glutamate (Fig. 2E and F) and LPS (Fig. 2G and H).

IPA significantly inhibited the wound closure of BV2 induced by LPS (0.1, 1.0, 10.0 and 100 μM IPA corresponded to 88.10±20.17, 91.55±28.29, 83.03±11.79 and 70.55±29.71%, respectively, compared with 146.60±7.19% migration area in the LPS group; Fig. 2I and J) and decreased LDH release (0.1, 1.0, 10.0 and 100.0 μM IPA doses corresponded to 352.93±72.37, 389.63±75.72, 319.76±40.31, and 244.11±31.44, respectively, compared with 495.12±47.63 U/l in the LPS group; Fig. 2K).

IPA suppresses LPS-induced apoptosis in BV2 cells. Treatment with IPA in the range of 0.1-100.0 μM prevented the LPS-induced late phase of apoptosis (LPS, 9.94±6.05%; 0.1 μM, 3.47±1.30%; 1 μM, 4.19±1.58%; 10 μM, 4.40±2.10%; 100 μM, 4.33±2.88%; Fig. 3A-C). It was confirmed by MMP that BV2 cells treated with IPA showed decreased JC-1 monomers compared with the LPS group (Fig. 3D).

IPA suppresses mRNA expression of anti-oxidative genes including superoxide dismutase(SOD)-1 and SOD-2, inflammatory genes (IL-1β and TNF-α) and M2-polarization genes (Arg-1) in LPS-treated BV2 cells. To explore the mechanism of action of IPA, mRNA expression of SOD-1 and SOD-2, which indicate ROS overload (35), was assessed. IPA at concentrations of 1, 10, and 100 μM significantly increased mRNA expression of SOD-1 and

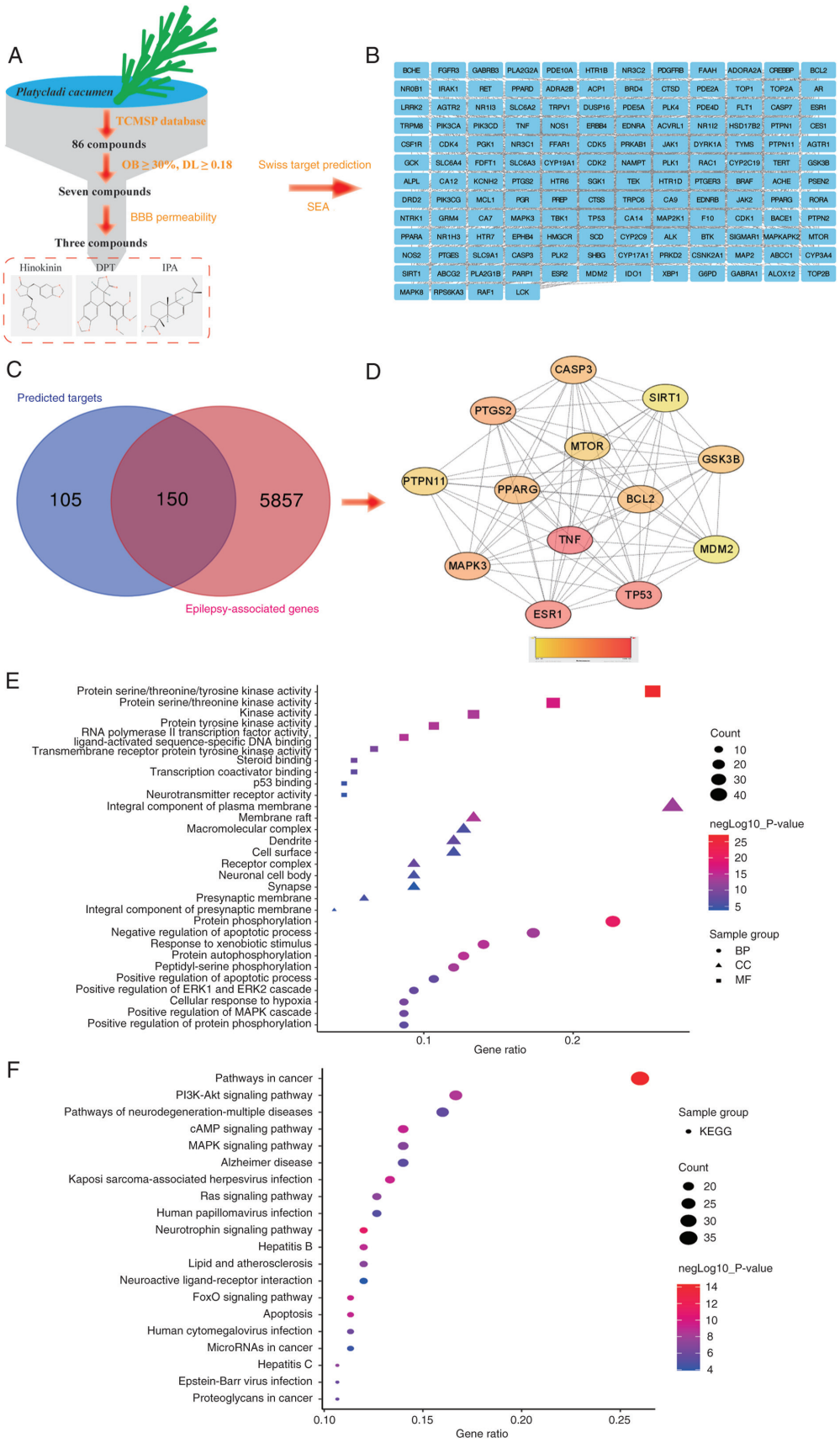

Figure 1. Network pharmacological study on the anti-epileptic effect of *Platycadi cacumen*. (A) Analysis of druggable compounds. A total of 86 compounds were obtained from TCMSP database, of which seven fulfilled the criteria OB ≥30% and DL ≥0.18. Hinokinin, DPT and IPA were predicted to cross BBB. (B) Predicted targets of hinokinin, DPT and IPA from SwissTarget and SEA database. (C) Venn diagram of overlapping target genes of compounds and epilepsy-associated genes. (D) Hub gene analysis by CytoNCA of 150 overlapping genes. (E) GO functional enrichment from 150 overlapping genes. (F) Pathways analysis of 50 overlapping genes. TCMSP, Traditional Chinese Medicine System Pharmacology Database; OB, oral bioavailability; DL, drug-likeness; DL, deoxypicropodophyllotoxin; IPA, isopimaric acid; BBB, blood-brain barrier; SEA, similarity ensemble approach; BP, biological processes; CC, cellular component; MF, molecular function; KEGG, Kyoto Encyclopedia of Genes and Genomes; GO, Gene Ontology.

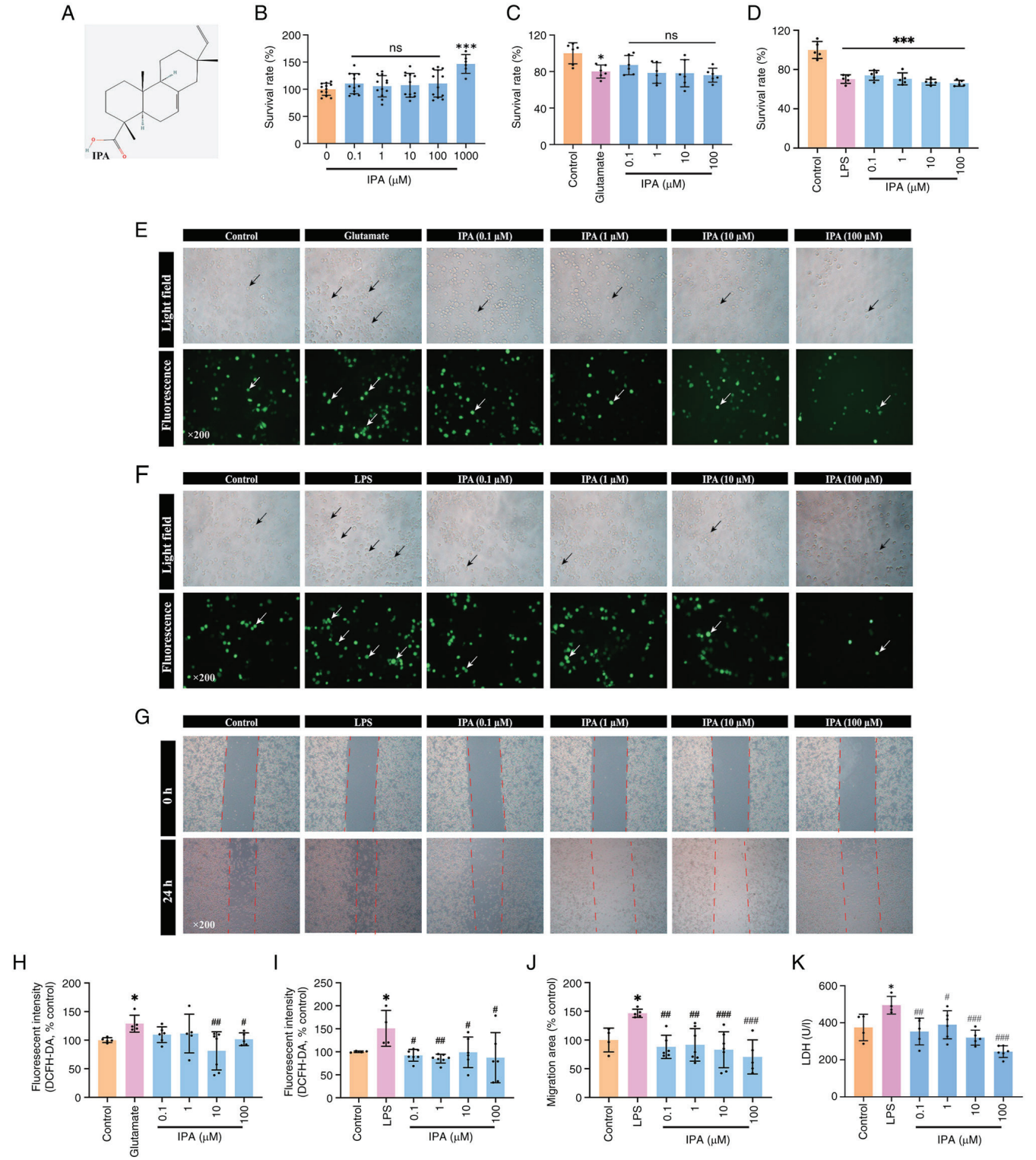

Figure 2. Anti-epileptic effects of IPA in LPS-induced BV2 cells. (A) Compound structure of IPA. (B) Survival rate of BV2 cells treated in the presence or absence of IPA for 24 h, compared with the 0 μM group. (C) Survival rate of BV2 cells treated with glutamate without or with IPA for 12 h. (D) Survival rate of BV2 cells treated with LPS without or with IPA for 24 h. (E) DCFH staining of the BV2 cells induced by glutamate without or with IPA for 12 h. (F) DCFH staining of the BV2 cells induced by LPS without or with IPA for 24 h. (G) Migration of BV2 cells induced by LPS without or with IPA for 24 h. (H) Analysis of ROS content in BV2 cells induced by glutamate without or with IPA. (I) ROS content in BV2 cells induced by LPS in the presence or absence of IPA. (J) Migration area and (K) LDH release of BV2 cells induced by LPS in the presence or absence of IPA. n=4-7. *P<0.05, ***P<0.001 vs. control; $^{\#}$P<0.05, $^{\#\#}$P<0.01, $^{\#\#\#}$P<0.001 vs. LPS or glutamate group. IPA, isopimaric acid; LPS, lipopolysaccharide; ROS, reactive oxygen species; LDH, Lactic dehydrogenase; ns, no significance.

SOD-2 (Fig. 4A and B). LPS induced significant increases of the mRNA expression of inflammatory genes including *IL-1*β (Fig. 4C) and *TNF-α* (Fig. 4D), while 100 μM of IPA significantly decreased the mRNA expression of *IL-1*β and *TNF-α*. Furthermore, it was demonstrated that LPS suppressed the mRNA expression of *Arg-1*, a specific

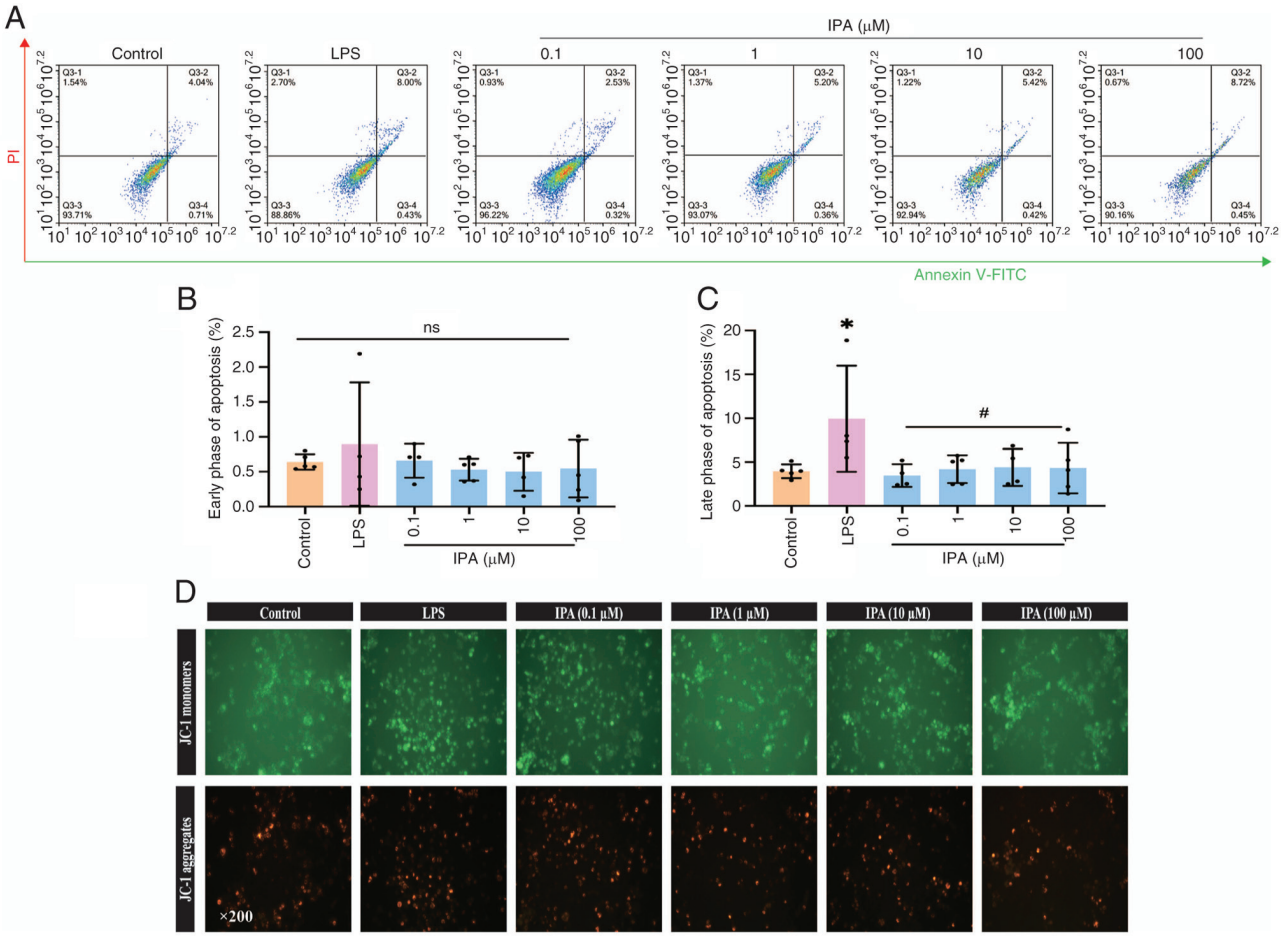

Figure 3. IPA inhibits LPS-induced late apoptosis of BV2 cells. (A) Representative flow cytometry. (B) Early and (C) late apoptotic rate. (D) Representative JC-1 staining. n=4 or 5. *P<0.05 vs. control; #P<0.05 vs. LPS. IPA, isopimaric acid; LPS, lipopolysaccharide; ns, no significance.

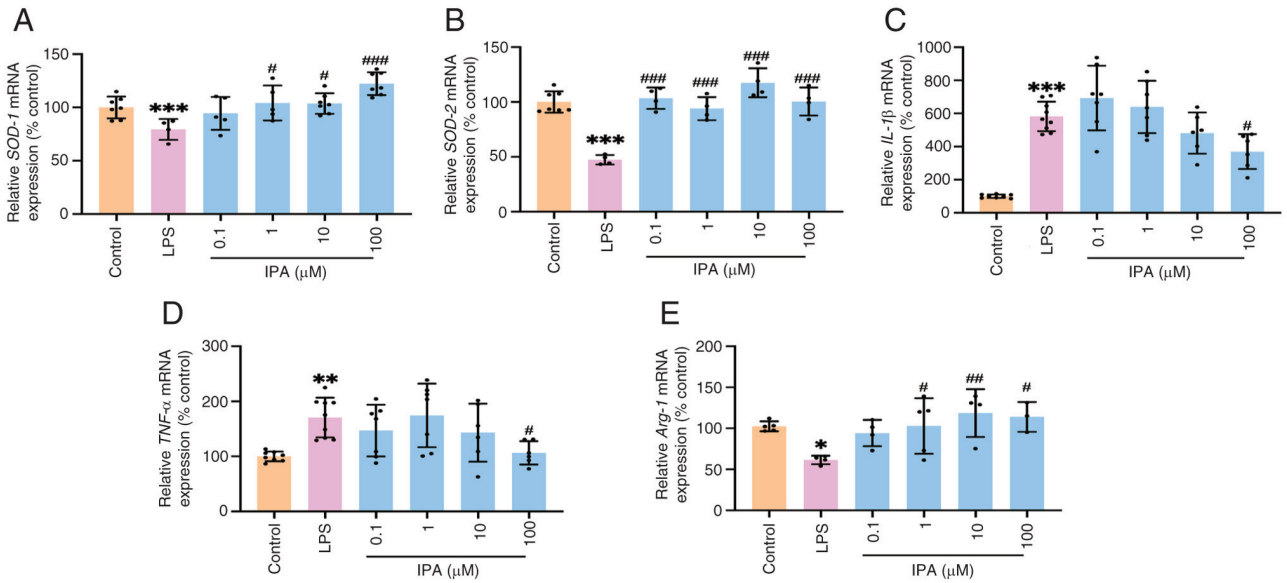

Figure 4. mRNA expression of genes associated with anti-oxidation, inflammation and polarization. mRNA expression of (A) SOD-1(B) SOD-2 (C) IL-1β, (D) TNF-α and (E) Arg-1. n=3-9, *P<0.05, **P<0.01, ***P<0.001 vs. control; #P<0.05, ##P<0.01 ###P<0.001 vs. LPS. SOD, superoxide dismutase; Arg, arginase; IPA, isopimaric acid; LPS, lipopolysaccharide.

surface phenotype marker of M2 (36). IPA at concentrations of 1, 10, and 100 μM significantly increased the mRNA expression of *Arg-1*, indicating that IPA induced the polarization of BV2 to M2 (Fig. 4E).

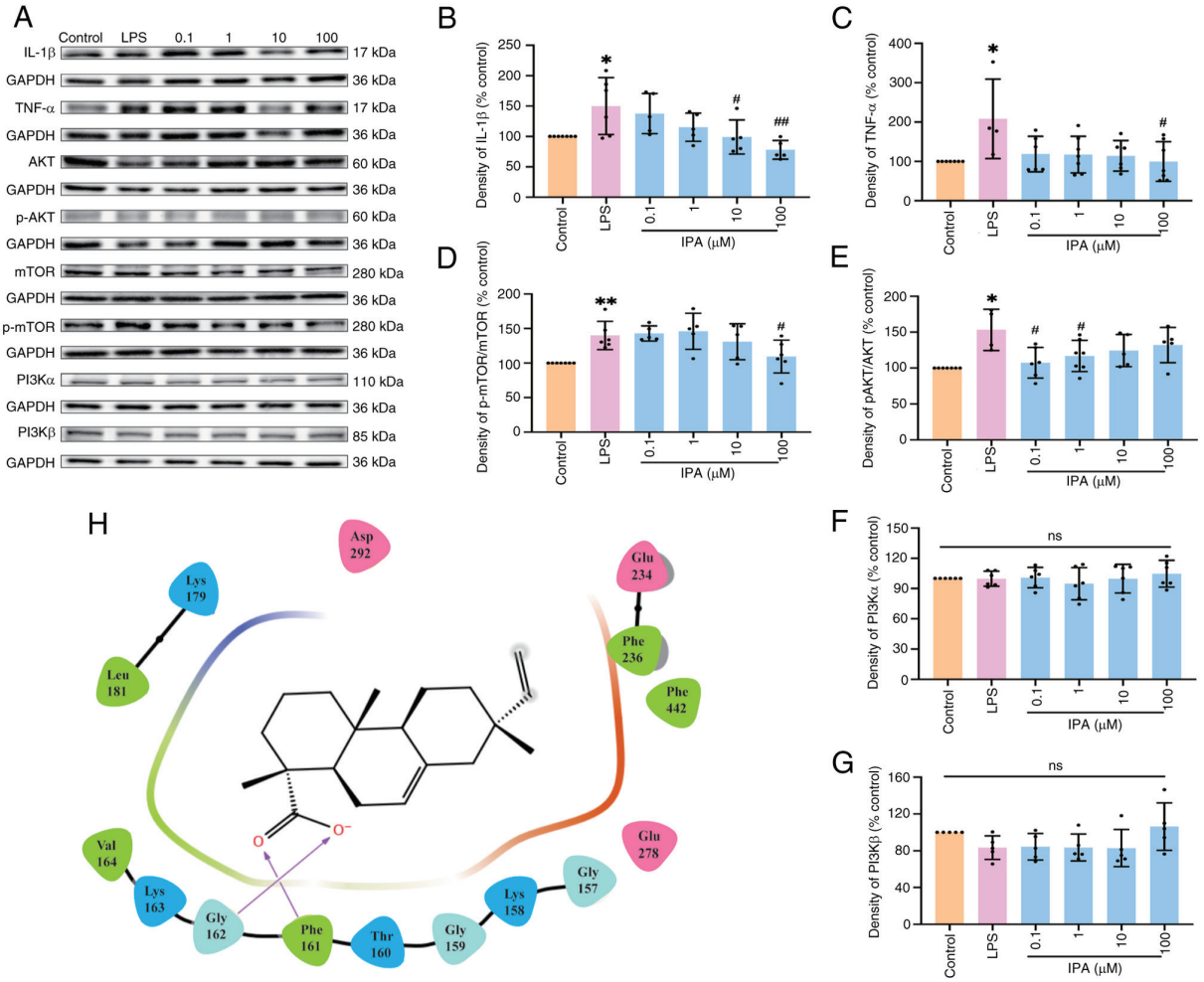

Figure 5. Protein expression of potential targets. (A) Representative blots for IL-1β, TNF-α, AKT, p-AKT, mTOR, p-mTOR, PI3Kα and PI3Kβ. Protein expression analysis of (B) IL-1β (C) TNF-α, (D) ratio of mTOR and p-mTOR, (E) ratio ofAKT and p-AKT, (F) PI3Kα and (G) PI3Kβ. (H) Binding model of IPA with active pocket of AKT. n=4-7, *P<0.05, **P<0.01 vs. control; $^{\#}$P<0.05, $^{\#\#}$P<0.01 vs. LPS. IPA, isopimaric acid; LPS, lipopolysaccharide; PI3K, phosphatidylinositol 3-kinase; p-, phosphorylation.

IPA suppresses protein expression of IL-1β and TNF-α by inhibiting the phosphorylation of hyperactive mTOR and AKT. Protein expression of hub (TNF-α and mTOR) and PI3K/AKT signaling pathway genes (AKT and p-AKT; Fig. 5A) were assessed. IPA inhibited protein expression of IL-1β (Fig. 5B) and TNF-α (Fig. 5C) compared with the LPS group. IPA also suppressed phosphorylation of mTOR (Fig. 5D) and AKT (Fig. 5E) but not of phosphatidylinositol 3-kinase (PI3K) α and β (Fig. 5F and G). Furthermore, molecular docking results confirmed that two oxygen atoms of carboxyl in IPA docked on the key Phe161 and Gly162 residue of AKT, which may interrupt the phosphorylation of AKT (37) (Fig. 5H).

Discussion

A total of ~40 antiepileptic drugs have been used to treat epileptic patients in clinical settings (38). However, most control the occurrence of acute seizures and do not exert a true antiepileptogenic effect. Currently, ~30% of patients with epilepsy experience uncontrollable seizures (39). Therefore, exploring novel antiepileptic drugs that impede epileptogenesis is vital for treating refractory epilepsy. Chinese herbal medicines including *Gastrodia elata, Uncaria rhynchophylla, Acrori tatarinowii, Paeonia lactiflora, Bupleurum Chinese* and PC have been used to treat seizures and epilepsy for thousands of years (40-42). The present study demonstrated that three compounds from PC, hinokinin, DPT and IPA showed druggability in crossing the BBB. In total, 150 predicted targets were associated with epilepsy, suggesting that hinokinin, DPT and IPA are potential components of PC against epilepsy.

Microglia are the primary glial cells in the central nervous system and act as immune protectors to maintain stability of the nerve cell microenvironment. Upon abnormal stimulation, microglia are transformed, exhibiting cellular structures varying from ramified to amoeboid, and enhancing migration to the injured region (43), where they induce release of inflammatory cytokines (IL-1β and TNF-α), and cause inflammation (44). Microglial activation and inflammation have been observed in the brain of patients with refractory epilepsy (45,46), which increases neuronal excitability and contributes to epileptogenesis (47). In the present study, IPA, a diterpenoid compound separated from PC (48), alleviated glutamate- and LPS-induced oxidative stress and inflammation in BV2 cells, confirming previous studies where IPA not only inhibited production of inflammation protein NF-κB in HBEC3-KT (*Homo sapiens* lung and bronchial epithelial

cells), MRC-5 (*Homo sapiens* lung fibroblasts), and THP-1 cells (*Homo sapiens* peripheral blood monocyte) (49), but also suppressed the proliferation and metastasis of breast cancer cells including (MDA-MB-231 and MCF-7) via mitochondrial oxidative phosphorylation signaling pathways (50). In particular, IPA significantly increased mRNA expression of anti-oxidative kinases (SOD-1 and SOD-2) and decreased gene expression of inflammatory factors (IL-1β and TNF-α), suggesting an anti-inflammation role in microglia.

An increasing number of studies have confirmed that hyperactive mTOR is involved in inflammation and apoptosis of microglia during epileptogenesis and is a potential target for epileptic treatment (51,52). Somatic mTOR variants, including p.C1483Y and p.C1483R, have been identified in patients with refractory epilepsy and focal cortical malformation (53), while, kainic acid- and LPS-induced seizures significantly activate mTOR in rats (54,55). The activation of mTOR in microglia enhances inflammatory responses (56). Furthermore, the PI3K/Akt pathway is key for mTOR-involved cell survival and migration (57,58). The present study demonstrated that IPA significantly inhibited phosphorylation of mTOR, confirming a previous study showing that inhibiting the PI3K/Akt/mTOR pathway prevents microglial apoptosis (59). As previous studies have demonstrated that protein expression of PI3Kα and β is significantly increased in acute and chronic epilepsy, independent of phosphorylation levels (60,61), the present study only analyzed the protein expression of PI3Kα and β. However, the present study did not find any changes to PI3Kα and β. Further analysis by molecular docking suggested that IPA may directly combine with AKT at the Phe161 and Gly162 residues and suppress activation of AKT, in line with a previous study that demonstrated residue Phe161 serves a vital role on AKT (37). Overall, the present study suggested that IPA inhibited LPS-induced neuroinflammation via the Akt/mTOR pathway. However, lack of data on the selectivity and specificity of IPA for AKT and mTOR in anti-epileptic activity is a limitation of the present study. Hence, their direct association should be investigated in the future.

In summary, IPA may be a potential anti-epileptic compound in PC that acts by suppressing neuroinflammation, apoptosis and polarization via the Akt/mTOR pathway. These findings indicate that IPA may be a novel anti-epileptic drug.

Acknowledgements

The authors would like to thank Dr Junyu Xu (Hainan Medical University, Haikou, China) for help with molecular docking.

Funding

The present study was supported by the Hainan Provincial Key Research and Development Program (grant nos. ZDYF 2021SHFZ092 and ZDYF2022SHFZ109); Hainan Provincial Natural Science Foundation of China (grant no. 820RC630); Epilepsy Research Science Innovation Group of Hainan Medical University (grant no. 2022); Hainan Province Clinical Medical Center (grant no. 2021); Excellent Talent Team of Hainan Province (grant no. QRCBT202121) and National Natural Science Foundation of China (grant nos. 81960249, 82260270 and 82360838).

Availability of data and materials

The data generated in the present study may be requested from the corresponding author.

Authors' contributions

YaW conceived and designed the study, analyzed data, wrote the manuscript and constructed figures. YuW, CL and DL designed the experiments. YuW performed experiments and constructed figures. YaW, YC, and QL confirm the authenticity of all the raw data. YC and QL designed the experiment, wrote the manuscript, and supervised the study. All authors have read and approved the final manuscript.

Ethics approval and consent to participate

Not applicable.

Patient consent for publication

Not applicable.

Competing interests

The authors declare that they have no competing interests.

References

1. Asadi-Pooya AA, Brigo F, Lattanzi S and Blumcke I: Adult epilepsy. Lancet 402: 412-424, 2023.
2. Pitkanen A, Ekolle Ndode-Ekane X, Lapinlampi N and Puhakka N: Epilepsy biomarkers-Toward etiology and pathology specificity. Neurobiol Dis 123: 42-58, 2019.
3. Chinese Pharmacopoeia Commission: Pharmacopoeia of the People's Republic of China. Vol 1. China Medical Science and Technology Press, Beijing, pp292-293, 2015.
4. Zhang ML, Liu YH and Qu HH: Protective effect of nanoparticles from *Platycladi cacumen* carbonisata on 2,4,6-Trinitrobenzene Sulfonic Acid (TNBS)-Induced Colitis in Rats. J Biomed Nanotechnol 18: 422-434, 2022.
5. Zhang HX, Li YY, Liu ZJ and Wang JF: Quercetin effectively improves LPS-induced intestinal inflammation, pyroptosis, and disruption of the barrier function through the TLR4/NF-κB/NLRP3 signaling pathway in vivo and in vitro. Food Nutr Res 66: 8948, 2022.
6. Fu H, Li W, Weng Z, Huang Z, Liu J, Mao Q and Ding B: Water extract of *cacumen platycladi* promotes hair growth through the Akt/GSK3beta/beta-catenin signaling pathway. Front Pharmacol 14: 1038039, 2023.
7. Zhang Y, Chen S, Qu F, Su G and Zhao Y: In vivo and in vitro evaluation of hair growth potential of *Cacumen Platycladi*, and GC-MS analysis of the active constituents of volatile oil. J Ethnopharmacol 238: 111835, 2019.
8. Huo X, Meng Q, Wang C, Wu J, Zhu Y, Sun P, Ma X, Sun H and Liu K: Targeting renal OATs to develop renal protective agent from traditional Chinese medicines: Protective effect of Apigenin against Imipenem-induced nephrotoxicity. Phytother Res 34: 2998-3010, 2020.
9. Zhuang B, Bi ZM, Wang ZY, Duan L, Lai CJ and Liu EH: Chemical profiling and quantitation of bioactive compounds in *Platycladi Cacumen* by UPLC-Q-TOF-MS/MS and UPLC-DAD. J Pharm Biomed Anal 154: 207-215, 2018.
10. Ding M, Li J, Zou S, Tang G, Gao X and Chang YX: Simultaneous extraction and determination of compounds with different polarities from *Platycladi cacumen* by AQ C(18)-Based vortex-homogenized matrix solid-phase dispersion with ionic liquid. Front Pharmacol 9: 1532, 2019.
11. Shen Y, Shen X, Cheng Y and Liu Y: Myricitrin pretreatment ameliorates mouse liver ischemia reperfusion injury. Int Immunopharmacol 89 (Pt A): 107005, 2020.

12. Oh TW, Do HJ, Jeon JH and Kim K: Quercitrin inhibits platelet activation in arterial thrombosis. Phytomedicine 80: 153363, 2021.
13. Qiu S, Zhou Y, Kim JT, Bao C, Lee HJ and Chen J: Amentoflavone inhibits tumor necrosis factor-alpha-induced migration and invasion through AKT/mTOR/S6k1/hedgehog signaling in human breast cancer. Food Funct 12: 10196-10209, 2021.
14. Zhang T (ed): Effective Prescription for Treating Epilepsy. 1st edition. People's Military Medical Press, Beijing, 1996 (In Chinese).
15. Wang Y, Li C, Xiong Z, Chen N, Wang X, Xu J, Wang Y, Liu L, Wu H, Huang C, *et al*: Up-and-coming anti-epileptic effect of aloesone in Aloe vera: Evidenced by integrating network pharmacological analysis, in vitro, and in vivo models. Front Pharmacol 13: 962223, 2022.
16. Tang Y, Li M, Wang J, Pan Y and Wu FX: CytoNCA: A cytoscape plugin for centrality analysis and evaluation of protein interaction networks. Biosystems 127: 67-72, 2015.
17. Sherman BT, Hao M, Qiu J, Jiao X, Baseler MW, Lane HC, Imamichi T and Chang W: DAVID: a web server for functional enrichment analysis and functional annotation of gene lists (2021 update). Nucleic Acids Res 50(W1): W216-W221, 2022.
18. Wang J, Sun Y, Zhang X, Cai H, Zhang C, Qu H, Liu L, Zhang M, Fu J, Zhang J, *et al*: Oxidative stress activates NORAD expression by H3K27ac and promotes oxaliplatin resistance in gastric cancer by enhancing autophagy flux via targeting the miR-433-3p. Cell Death Dis 12: 90, 2021.
19. Wang Y, Li Y, Liu D, Zheng D, Li X, Li C, Huang C, Wang Y, Wang X, Li Q and Xu J: A potential anti-glioblastoma compound LH20 induces apoptosis and arrest of human glioblastoma cells via CDK4/6 inhibition. Molecules 28: 5047, 2023.
20. Wang Y, Li Y, Wang G, Lu J and Li Z: Overexpression of Homer1b/c induces valproic acid resistance in epilepsy. CNS Neurosci Ther 29: 331-343, 2023.
21. Wang Y, Xiong Z, Li C, Liu D, Li X, Xu J, Chen N, Wang X, Li Q and Li Y: Multiple beneficial effects of aloesone from aloe vera on LPS-Induced RAW264.7 cells, including the inhibition of oxidative stress, inflammation, M1 polarization, and apoptosis. Molecules 28: 1617, 2023.
22. Livak KJ and Schmittgen TD: Analysis of relative gene expression data using real-time quantitative PCR and the 2(-Delta Delta C(T)) Method. Methods 25: 402-408, 2001.
23. Addie M, Ballard P, Buttar D, Crafter C, Currie G, Davies BR, Debreczeni J, Dry H, Dudley P, Greenwood R, *et al*: Discovery of 4-amino-N-[(1S)-1-(4-chloro phenyl)-3-hydroxypropyl]-1-(7H-pyrrolo[2,3-d]pyrimidin-4-yl) piperidine-4-carboxamide (AZD5363), an orally bioavailable, potent inhibitor of Akt kinases. J Med Chem 56: 2059-2073, 2013.
24. Yang Y, Yao K, Repasky MP, Leswing K, Abel R, Shoichet BK and Jerome SV: Efficient Exploration of Chemical Space with Docking and Deep Learning. J Chem Theory Comput 17: 7106-7119, 2021.
25. Xu J, Li H, Wang X, Huang J, Li S, Liu C, Dong R, Zhu G, Duan C, Jiang F, *et al*: Discovery of coumarin derivatives as potent and selective cyclin-dependent kinase 9 (CDK9) inhibitors with high antitumour activity. Eur J Med Chem 200: 112424, 2020.
26. Ying J, Huang Y, Ye X, Zhang Y, Yao Q, Wang J, Yang X, Yu C, Guo Y, Zhang X, *et al*: Comprehensive study of clinicopathological and immune cell infiltration and lactate dehydrogenase expression in patients with thymic epithelial tumours. Int Immunopharmacol 126: 111205, 2024.
27. Smith E, Williamson E, Zloh M and Gibbons S: Isopimaric acid from Pinus nigra shows activity against multidrug-resistant and EMRSA strains of Staphylococcus aureus. Phytother Res 19: 538-542, 2005.
28. Wu XW, Wang Q, Li Q, Cui YM, Pu YK, Shi QQ, Bi DW, Zhang JJ, Zhang RH, Li XL, *et al*: Rubellawus A-D, four new diterpenoids isolated from callicarpa rubella and Their Anti-NLRP3 inflammasome effects. Chem Biodivers 17: e2000798, 2020.
29. Yamamoto K, Ueta Y, Wang L, Yamamoto R, Inoue N, Inokuchi K, Aiba A, Yonekura H and Kato N: Suppression of a neocortical potassium channel activity by intracellular amyloid-beta and its rescue with Homer1a. J Neurosci 31: 11100-11109, 2011.
30. Wang L, Kang H, Li Y, Shui Y, Yamamoto R, Sugai T and Kato N: Cognitive recovery by chronic activation of the large-conductance calcium-activated potassium channel in a mouse model of Alzheimer's disease. Neuropharmacology 92: 8-15, 2015.
31. Salari S, Silvera Ejneby M, Brask J and Elinder F: Isopimaric acid-a multi-targeting ion channel modulator reducing excitability and arrhythmicity in a spontaneously beating mouse atrial cell line. Acta Physiol (Oxf) 222: e12895, 2018.
32. Imaizumi Y, Sakamoto K, Yamada A, Hotta A, Ohya S, Muraki K, Uchiyama M and Ohwada T: Molecular basis of pimarane compounds as novel activators of large-conductance Ca(2+)-activated K(+) channel alpha-subunit. Mol Pharmacol 62: 836-846, 2002.
33. Zaugg J, Khom S, Eigenmann D, Baburin I, Hamburger M and Hering S: Identification and characterization of GABA(A) receptor modulatory diterpenes from *Biota orientalis* that decrease locomotor activity in mice. J Nat Prod 74: 1764-1772, 2011.
34. Rong S, Wan D, Fan Y, Liu S, Sun K, Huo J, Zhang P, Li X, Xie X, Wang F and Sun T: Amentoflavone affects epileptogenesis and exerts neuroprotective effects by inhibiting NLRP3 inflammasome. Front Pharmacol 10: 856, 2019.
35. Chang YC, Fong Y, Tsai EM, Chang YG, Chou HL, Wu CY, Teng YN, Liu TC, Yuan SS and Chiu CC: Exogenous C(8)-Ceramide Induces Apoptosis by Overproduction of ROS and the switch of superoxide dismutases SOD1 to SOD2 in human lung cancer cells. Int J Mol Sci 19: 3010, 2018.
36. Xu M, Yang Y, Peng J, Zhang Y, Wu B, He B, Jia Y and Yan T: Effects of Alpinae Oxyphyllae Fructus on microglial polarization in a LPS-induced BV2 cells model of neuroinflammation via TREM2. J Ethnopharmacol 302(Pt A): 115914, 2023.
37. Kashyap MP, Singh AK, Kumar V, Yadav DK, Khan F, Jahan S, Khanna VK, Yadav S and Pant AB: Pkb/Akt1 mediates Wnt/GSK3β/β-catenin signaling-induced apoptosis in human cord blood stem cells exposed to organophosphate pesticide monocrotophos. Stem Cells Dev 22: 224-238, 2013.
38. Ravizza T, Scheper M, Di Sapia R, Gorter J, Aronica E and Vezzani A: mTOR and neuroinflammation in epilepsy: Implications for disease progression and treatment. Nat Rev Neurosci 25: 334-350, 2024.
39. Janson MT and Bainbridge JL: Continuing burden of refractory epilepsy. Ann Pharmacother 55: 406-408, 2021.
40. Lin CH and Hsieh CL: Chinese herbal medicine for treating epilepsy. Front Neurosci 15: 682821, 2021.
41. Lu H, Luo M, Chen R, Luo Y, Xi A, Wang K and Xu Z: Efficacy and safety of traditional Chinese medicine for the treatment of epilepsy: A updated meta-analysis of randomized controlled trials. Epilepsy Res 189: 107075, 2023.
42. Wu J, Cao M, Peng Y, Dong B, Jiang Y, Hu C, Zhu P, Xing W, Yu L, Xu R and Chen Z: Research progress on the treatment of epilepsy with traditional Chinese medicine. Phytomedicine 120: 155022, 2023.
43. Block ML, Zecca L and Hong JS: Microglia-mediated neurotoxicity: Uncovering the molecular mechanisms. Nat Rev Neurosci 8: 57-69, 2007.
44. Hernandez VG, Lechtenberg KJ, Peterson TC, Zhu L, Lucas TA, Bradshaw KP, Owah JO, Dorsey AI, Gentles AJ and Buckwalter MS: Translatome analysis reveals microglia and astrocytes to be distinct regulators of inflammation in the hyperacute and acute phases after stroke. Glia 71: 1960-1984, 2023.
45. Butler T, Li Y, Tsui W, Friedman D, Maoz A, Wang X, Harvey P, Tanzi E, Morim S, Kang Y, *et al*: Transient and chronic seizure-induced inflammation in human focal epilepsy. Epilepsia 57: e191-194, 2016.
46. Kumar P, Lim A, Hazirah SN, Chua CJH, Ngoh A, Poh SL, Yeo TH, Lim J, Ling S, Sutamam NB, *et al*: Single-cell transcriptomics and surface epitope detection in human brain epileptic lesions identifies pro-inflammatory signaling. Nat Neurosci 25: 956-966, 2022.
47. Luo C, Koyama R and Ikegaya Y: Microglia engulf viable newborn cells in the epileptic dentate gyrus. Glia 64: 1508-1517, 2016.
48. Cui X, Cheng L, Liu Q and Jia Y: Isolation, identification and HPLC analysis of active component isopimaric acid in leaves of *Platycladus orientalis*. Lishizhen Med Mater Med Res 15: 78-79, 2004 (In Chinese).
49. Michavila Puente-Villegas S, Apaza Ticona L, Rumbero Sanchez A and Acebes JL: Diterpenes of Pinus pinaster aiton with anti-inflammatory, analgesic, and antibacterial activities. J Ethnopharmacol 318(Pt B): 117021, 2024.
50. Li J, Liu X, Chen L, Zhu X, Yu Z, Dong L, Zhao X, Zou H, Wei Q, Feng Y, *et al*: Isopimaric acid, an ion channel regulator, regulates calcium and oxidative phosphorylation pathways to inhibit breast cancer proliferation and metastasis. Toxicol Appl Pharmacol 462: 116415, 2023.

51. Hodges SL and Lugo JN: Therapeutic role of targeting mTOR signaling and neuroinflammation in epilepsy. Epilepsy Res 161: 106282, 2020.
52. Hu Y, Mai W, Chen L, Cao K, Zhang B, Zhang Z, Liu Y, Lou H, Duan S and Gao Z: mTOR-mediated metabolic reprogramming shapes distinct microglia functions in response to lipopolysaccharide and ATP. Glia 68: 1031-1045, 2020.
53. Lai D, Gade M, Yang E, Koh HY, Lu J, Walley NM, Buckley AF, Sands TT, Akman CI and Mikati MA, *et al*: Somatic variants in diverse genes leads to a spectrum of focal cortical malformations. Brain 145: 2704-2720, 2022.
54. Huang XY, Hu QP, Shi HY, Zheng YY, Hu RR and Guo Q: Everolimus inhibits PI3K/Akt/mTOR and NF-kB/IL-6 signaling and protects seizure-induced brain injury in rats. J Chem Neuroanat 114: 101960, 2021.
55. Russo E, Andreozzi F, Iuliano R, Dattilo V, Procopio T, Fiume G, Mimmi S, Perrotti N, Citraro R, Sesti G, *et al*: Early molecular and behavioral response to lipopolysaccharide in the WAG/Rij rat model of absence epilepsy and depressive-like behavior, involves interplay between AMPK, AKT/mTOR pathways and neuroinflammatory cytokine release. Brain Behav Immun 42: 157-168, 2014.
56. Zhao XF, Liao Y, Alam MM, Mathur R, Feustel P, Mazurkiewicz JE, Adamo MA, Zhu XC and Huang Y: Microglial mTOR is neuronal protective and antiepileptogenic in the pilocarpine model of temporal lobe epilepsy. J Neurosci 40: 7593-7608, 2020.
57. Zhu F, Kai J, Chen L, Wu M, Dong J, Wang Q and Zeng LH: Akt inhibitor perifosine prevents epileptogenesis in a rat model of temporal lobe epilepsy. Neurosci Bull 34: 283-290, 2018.
58. Bai Q, Wang X, Yan H, Wen L, Zhou Z, Ye Y, Jing Y, Niu Y, Wang L, Zhang Z, *et al*: Microglia-Derived Spp1 promotes pathological retinal neovascularization via activating endothelial Kit/Akt/mTOR signaling. J Pers Med 13: 146, 2023.
59. Du M, Sun Z, Lu Y, Li YZ, Xu HR and Zeng CQ: Osthole inhibits proliferation and induces apoptosis in BV-2 microglia cells in kainic acid-induced epilepsy via modulating PI3K/AKt/mTOR signalling way. Pharm Biol 57: 238-244, 2019.
60. Xiao Z, Peng J, Gan N, Arafat A and Yin F: Interleukin-1β plays a pivotal role via the PI3K/Akt/mTOR signaling pathway in the chronicity of mesial temporal lobe epilepsy. Neuroimmunomodulation 23: 332-344, 2016.
61. Wang P, Nan S, Zhang Y and Fan J: Effects of GABA(B) receptor positive allosteric modulator BHF177 and IRS-1 on apoptosis of hippocampal neurons in rats with refractory epilepsy via the PI3K/Akt pathway. Cell Biol Int 46: 1775-1786, 2022.